이학박사 학위논문

Carbon Nanotube Devices for Monitoring the Activity of Thermoreceptors in Nanovesicles and Their Applications for Bioelectronic Skins

온도 수용체의 작용을 연구하기 위한 나노베지클-탄소나노튜브 장치 및 바이오전자 피부로의 응용

2020 년 2 월

서울대학교 대학원

물리천문학부 물리학 전공

신 나 래

Carbon Nanotube Devices for Monitoring the Activity of Thermoreceptors in Nanovesicles and Their Applications for Bioelectronic Skins

by

Narae Shin

Supervised by

Professor Seunghun Hong

A Dissertation Submitted to the Faculty of Seoul National University in Partial Fulfillment of the Requirements for the Degree of Doctor of Philosophy

February 2020

Department of Physics and Astronomy

Graduate School

Seoul National University

Abstract

Carbon Nanotube Devices for Monitoring the Activity of Thermoreceptors in Nanovesicles and Their Applications for Bioelectronic Skins

Narae Shin

Department of Physics and Astronomy

The Graduate School

Seoul National University

Human perceives changes in external environments such as odorants, tastants and temperature through olfactory, gustatory and somesthetic systems. Among them, tactile sensations are triggered when thermoreceptors in cells receive chemical signals or feel changes in temperatures from outside cells. In other words, thermoreceptors act as the first sensing parts in sensory systems. Therefore, the monitoring of thermoreceptor activity is essential for the fundamental understanding of somesthetic systems. In addition, the study on thermoreceptors may lead to the development of bioelectronic sensors. In this dissertation, it will be discussed about the electrically monitoring of thermoreceptor activity

via bioelectronic sensors. The bioelectronic sensors were based on carbon nanotube field effect transistors (CNT-FETs).

First, a bioelectronic skin based on nanovesicles for the monitoring of thermoreceptor activity to cool sensation will be discussed. Here, CNT-FETs were hybridized with nanovesicles containing human thermoreceptors, transient receptor potential melastatin 8 (hTRPM8). This method enabled us to discriminate between menthol, well-known cooling agent, and non-cooling substances with high sensitivity and selectivity. Interestingly, bioelectronic skins could also be used for the detection of menthol in real samples such as an electronic liquid menthol oil. Moreover, the enhancement of cool sensation by lower temperature (18℃) was demonstrated using this platform.

Next, a bioelectronic skin based on nanovesicles for the monitoring of human thermoreceptor activity to irritant substances and cold sensation will be discussed. In this strategy, a floating electrode-based CNT-FET was functionalized with nanovesicles containing human thermoreceptors, transient receptor potential ankyrin 1 (hTRPA1). This strategy allowed us to sensitively evaluate the contents of cinnamaldehyde, as low as 1 fM. Here, we also demonstrated that the responses of hTRPA1 to cinnamaldehyde could be enhanced by a lower temperature (10℃). Furthermore, the method provided a means to

quantitatively evaluate cinnamaldehyde in real samples such as cinnamon massage oil.

Keywords: thermoreceptor, nanovesicle, carbon nanotube field effect transistor, floating electrode, bioelectronic skin

Student Number: 2015-30092

Table of contents

List of figures

Chapter 1

Introduction

1.1 Thermoreceptor Protein

In human, the five senses are sight, hearing, smell, touch and taste. These senses play a unique role by receiving signal information from the external environments through the sense organs. Among them, the sense of touch appears through the skin; the skin detects pressure, pain, heat and cold, allowing us to perceive important information about our surroundings. The sense of touch is triggered when thermoreceptors in cells receive chemical signals or temperature changes from outside the cells. Such thermoreceptor proteins embedded in the plasma membrane of cells allow communications between inside and outside of the cells [1,2]. Signal transduction is triggered through these membrane receptors. Ion channel-linked receptors are the group of membrane receptors, and they open to allow ions to pass through membrane in response to the binding of ligands [3]. These membrane receptors exist somesthetic systems [4]. They have been widely studied because they can provide fundamental understanding of sensory systems such as somesthetic systems. In addition, the study on thermoreceptors can lead to the development of bioelectronic skins.

1.2 Monitoring of Thermoreceptor Protein Activity

The monitoring of receptor activity has previously been studied by using cell-based assays [5]. For example, in respect of a fluorescence assay, cells expressing receptor proteins are cultured, and treated with fluorescence indicators. Then, the activity of receptor proteins can be monitored by measuring a fluorescence intensity [6]. In point of a luciferase assay, receptor proteins and luciferase genes are transfected in cells. When certain ligands bind to the receptor proteins, signal transduction is triggered, resulting in the expression of luciferase genes [7]. The receptor activity can be monitored by measuring a luminescence intensity in cells. However, these methods are complicated and difficult to manipulate. In addition, it is hard to monitor the activity of receptor proteins sensitively.

To get over these problems, the methods using bioelectronic sensors have been widely studied. When certain ligands bind to their specific receptors, biological signals are generated. The biological signals can be converted into electrical signals by sensor transducers [8]. Some processors allow one to measure electrical signals such as conductance (Figure 1-1). Further, many studies have been conducted to develop bioelectronic sensors using biological recognition elements such as receptor proteins [9]. For example, bioelectronic sensors using

conventional carbon nanotube field effect transistors (CNT-FETs) as a transducer have been developed to monitor the activity of receptor proteins [9,10].

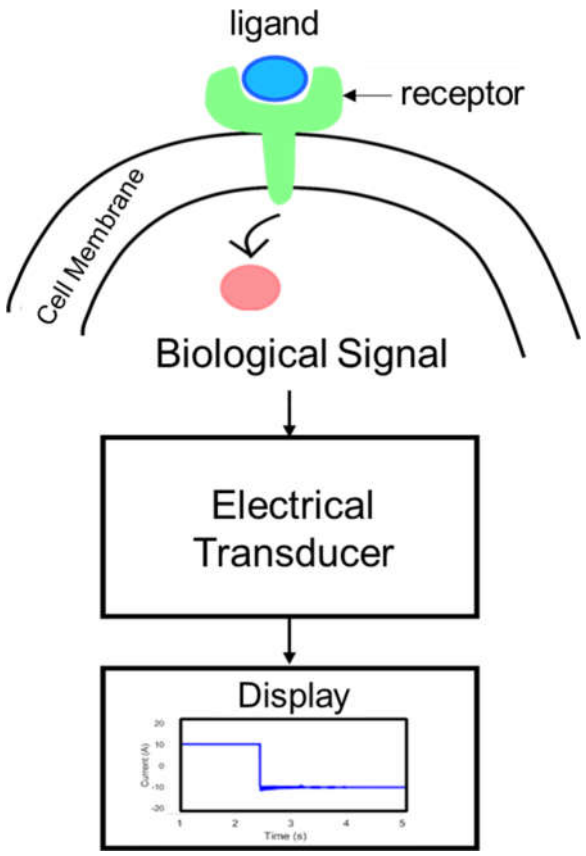

Figure 1-1 Schematic diagram representing the electrical monitoring of binding signals between receptors and ligands. When specific ligands bind to their receptors, biological signals occur. The biological signals can be converted into electrical signals through a sensor transducer. One can monitor electrical signals such as conductance after some processing.

1.3 Carbon Nanotube Field Effect Transistor

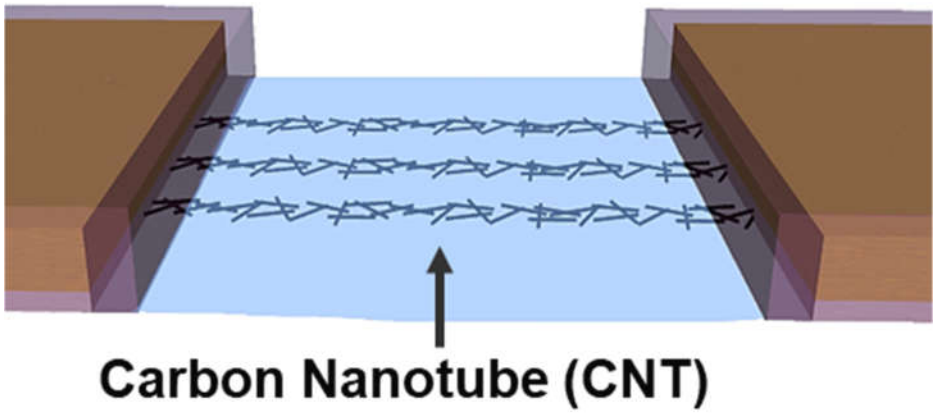

Figure 1-2 Schematic diagram showing a conventional CNT-FET. CNTs were selectively assembled onto a SiO_2 substrate. Source and drain electrodes were fabricated *via* photolithography and thermal evaporation methods. A passivation layer was formed onto the source and drain electrodes.

The performance of bioelectronic sensors depend on the efficiency of a transducer, since the sensitivity and selectivity of sensors are primarily determined by a transducer. A transducer based on CNT-FET were previously studied due to its high electrical conductivity (Figure 1-2) [11]. The CNT-FET showed high performance as a bioelectronic sensor than cell-based assays. Receptor proteins are immobilized on CNT channels, and the direct binding events of specific target molecules occur on the CNT channels, resulting in high selectivity and sensitivity [12,13]. In addition, CNT-FETs could be fabricated on a wafer scale by

conventional methods such as photolithography and thermal evaporation methods. Thus, bioelectronic sensors based on CNT-FETs can be powerful tools, and are considered as a way to study sensory systems for various practical applications.

1.4 References

[1] Grecco, H. E.; Schmick, M.; Bastiaens, P. I. H. *Cell* **2011,** *144*, 897-909.

[2] Rosenbaum, D. M.; Rasmussen, S. G.; Kobilka, B. K. *Nature* **2009,** *459*, 356-363.

[3] Kang, N.; Koo, J. *BMB Rep.* **2012,** *45*, 612-622.

[4] Jacoby, E.; Bouhelal, R.; Gerspacher, M.; Seuwen, K. *ChemMedChem* **2006,** *1*, 761-782.

[5] Absalom, N. L.; Lewis, T. M.; Schofield, P. R. *Exp. Physiol.* **2004,** *89*, 145-153.

[6] Su, J. L.; Fornwald, J.; Rivers, P.; Goldsworthy, S.; Looney, N. A.; Hanvey, J.; Plumpton, C.; Parham, J.; Romanos, M.; Kost, T. A.; Kull, F. C. *J. Immunol. Methods* **2004,** *291*, 123-135.

[7] Zhuang, H.; Matsunami, H. *Nat. Protoc.* **2008,** *3*, 1402-1413.

[8] Perumal, V.; Hashim, U. *J. Appl. Biomed.* **2014,** *12*, 1-15.

[9] Dung, T. T.; Oh, Y.; Choi, S. J.; Kim, I. D.; Oh, M. K.; Kim, M. *Sensors* **2018,** *18*, 103.

[10] Kim, T. H.; Lee, S. H.; Lee, J.; Song, H. S.; Oh, E. H.; Park, T. H.; Hong, S. *Adv. Mater.* **2009,** *21*, 91-94.

[11] Lee, J.; Lee, H.; Kim, T.; Jin, H. J.; Shin, J.; Shin, Y.; Park, S.; Khang, Y.; Hong, S. *Nanotechnology* **2012,** *23*, 085204.

[12] Kim, B.; Lee, J.; Namgung, S.; Kim, J.; Park, J. Y.; Lee, M. S.;

Hong, S. *Sens. Actuators, B* **2012,** *169*, 182-187.

[13] Ta, V. T.; Park, J.; Park, E. J.; Hong, S. *ACS Nano* **2014,** *8*, 2206-2213.

Chapter 2

Bioelectronic Skin based on Nanovesicles for the Monitoring of Human Thermoreceptor Activity to Cool Sensation

2.1 Introduction

In human, a somesthetic sense comprises of versatile senses of temperature, pressure, and pain [1]. Humans rely on highly-efficient somesthetic systems in avoiding dangers and recognizing environmental changes, inspiring many researchers to build artificial sensory devices to mimic animal somesthetic systems. Previously, artificial somesthetic sensors have been primarily focused on thermosensors or mechanical, resulting in various practical applications such as touch pads and thermocouples [2-6]. Although the sense of cold is an important portion of somesthetic senses, only limited studies have been conducted for the development of a sensor to detect cold stimuli. For instance, analytical methods like cell-based assays and electric potential measurements have been utilized for the detection of cool stimuli, the chemical species stimulating chemical cool sensation, such as menthol [7-9]. However, cell-based assays are not suitable for developing artificial sensory devices because of their complicated pretreatment processes, tough manipulations, and a long measurement time. The feasibility of previous non-cell-based assays are still inferior to that of human temperature sensor systems in terms of its sensitivity and selectivity. On the other hand, hybrid nanostructures based on carbon nanotubes (CNTs) and receptor proteins have been utilized to develop artificial sensory devices

to imitate human noses or tongues [10-14]. However, such sensor devices to detect chemical cool stimuli have not been demonstrated yet.

In this dissertation, we built the hybrid structure of thermoreceptor proteins and single-walled carbon nanotube-based field effect transistors (CNT-FETs) that can respond to chemical cool stimuli such as human somesthetic systems. We expressed a human transient receptor potential melastatin 8 (hTRPM8), a receptor protein for chemical cool stimuli, in human embryonic kidney cell line 293T (HEK293T) cells, and nanovesicles produced from the cells were immobilized on CNT-FETs. In human, the TRPM8 is involved in the transmission and modulation of cool sensation [7-9,15,16]. In our sensor device, the nanovesicles containing the hTRPM8 protein responded to chemical cool stimuli, which was monitored directly *via* the underlying CNT channels of CNT-FETs. Our sensors could selectively detect chemical cool stimuli such as menthol at 1 nM concentration among other chemical stimuli. This is the first sensor device which allows us to quantitatively evaluate the chemical cool stimuli in real-time just like human sensory systems. Our sensor should be a powerful tool for a fundamental study regarding somesthetic systems, and it could be also used for various practical devices such as drug and food screening.

2.2 Fabrication of a Bioelectronic Skin Mimicking Human Somesthetic System

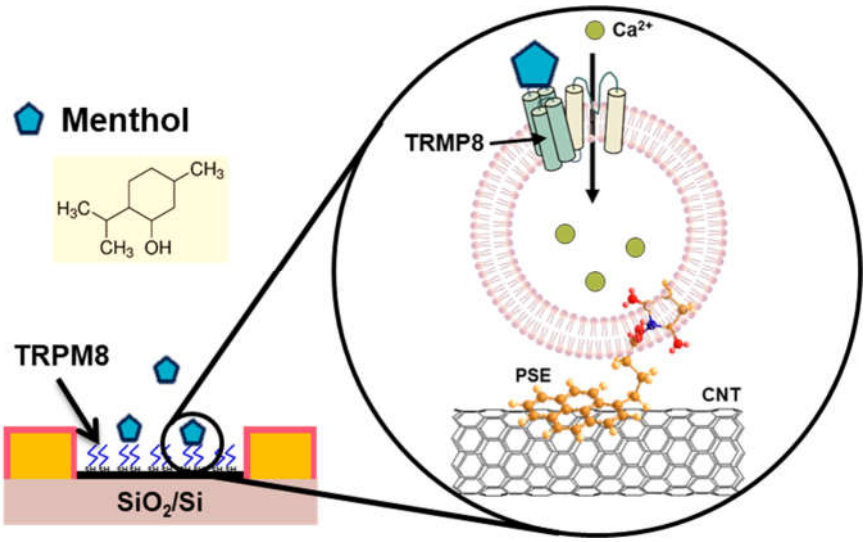

Figure 2-1 Schematic diagram depicting the fabrication process of a CNT-based bioelectronic skin mimicking human somesthetic systems. A CNT-FET was hybridized with nanovesicles containing human thermoreceptor, hTRPM8. The CNT-FET was fabricated *via* photolithography and thermal evaporation processes. The nanovesicles containing hTRPM8 were immobilized on the CNT channels of CNT-FETs. hTRPM8 can respond to specific chemical cool stimuli with high sensitivity and selectivity.

Figure 2-1 is a schematic diagram describing a hybrid structure of carbon nanotube sensor transducer and nanovesicles containing a thermoreceptor of human, hTRPM8. We fabricated a CNT-FET as described previously [17-20]. Briefly, CNTs were selectively adsorbed on a SiO_2 substrate, followed by the fabrication of source-drain

electrodes by thermal deposition. Finally, source and drain electrodes were covered by a passivation layer. It has been reported that a biosensor based on a CNT-FET exhibited high electrical performances than a conventional cell-based assays [20]. Following the fabrication of the CNT-FET, we immobilized nanovesicles containing hTRPM8 on the CNT channels of CNT-FETs. The hTRPM8, thermoreceptor, could recognize specific chemical cool stimuli such as menthol. Our fabrication methods allow us to mass-produce devices in a wafer scale. In this work, we could fabricate 24 devices on a single wafer and performed sensing experiments using four devices for each data point to confirm the reliability of our method.

2.3 Characterization of hTRPM8 in HEK-293T Cells and Nanovesicles

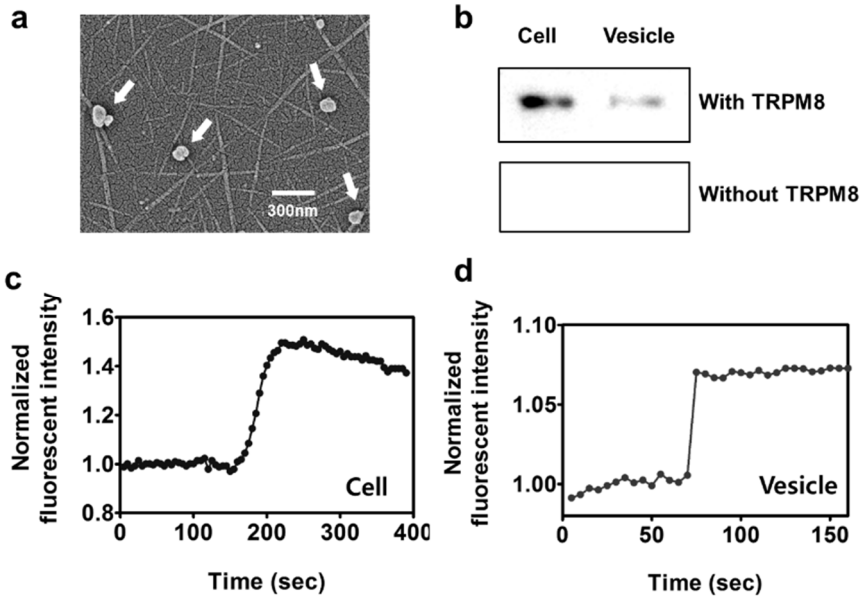

Figure 2-2 Expression of TRPM8 in HEK-293T cells and nanovesicles. (a) FE-SEM image of nanovesicles containing TRPM8 on CNT channels. (b) Western blot analysis of TRPM8 protein expression in HEK-293T cells and cell-derived nanovesicles. Transfected cells and nanovesicles with TRPM8 exhibited the specific band corresponding to the molecular weight of TRPM8, while control cells and nanovesicles (without TRPM8) did not show the band. (c) Real-time response of the calcium influx of cells in response to the addition of menthol. Only the addition of menthol caused Ca^{2+} influx in the HEK-293T cells. (d) Real-time measurement of Ca^{2+} assay in the nanovesicles containing TRPM8. The addition of 10 mM of menthol resulted in the increase of fluorescence intensity.

Figure 2-2a is the field emission scanning electron microscopy

(FE-SEM) image of nanovesicles immobilized on CNT channels. Before the SEM imaging, the nanovesicles were lyophilized to maintain their structures and then coated with 10 nm thick platinum using a sputter coater. This image shows that the nanovesicles could be immobilized uniformly on surfaces.

To confirm the expression of hTRPM8 in the cells and vesicles, western blot analysis was performed (Figure 2-2b). The cells expressing the hTRPM8 gene and nanovesicles showed bands at 120 kDa, corresponding to the molecular weight of hTRPM8. When the cells were transfected with mock vectors, or nanovesicles were produced from the cells, bands were not observed. Therefore, hTRPM8 channels were well-expressed on the surface of the cells and nanovesicles after transfection with a vector containing hTRPM8 [21,22].

Figure 2-2c shows a real-time profile of the calcium influx of cells in response to the addition of menthol. After the HEK-293 cells were transfected with vectors that contained the hTRPM8 gene, the calcium indicator, Fluo-4, was loaded into the cells. Upon menthol stimulation, the hTRPM8 channel opens and Ca^{2+} influx occurs. The Ca^{2+} influx through the hTRPM8 channel induced changes in the

fluorescence signal of the Fluo-4 dye. The changes were measured using a spectrofluorophotometer. When the cells expressing TRPM8 channels were stimulated with 1×10^{-3} M menthol, the fluorescence signals increased. This result indicated that the interaction between hTRPM8 channels and menthol induced Ca^{2+} influx into the cells. Therefore, hTRPM8 channels were expressed on the surface of cells, and the channels are functional and can recognize menthol.

Figure 2-2d shows the real-time change in fluorescence signals that are induced after Ca^{2+} influx into the nanovesicles containing hTRPM8 channels. After the Ca^{2+} indicator was loaded into the cells, nanovesicles were produced and immobilized on the bottom of a 96-well plate by poly-d-lysine. The nanovesicles were stimulated with 1×10^{-3} M menthol and the change in fluorescence signals were monitored. The nanovesicles containing the hTRPM8 channel showed an increase in fluorescence signals when stimulated by menthol. The results indicate that the nanovesicles containing the hTRPM8 channel are functional and can recognize menthol to induce the Ca^{2+} influx [23,24].

2.4 Responses of Bioelectronic Skins to Menthol

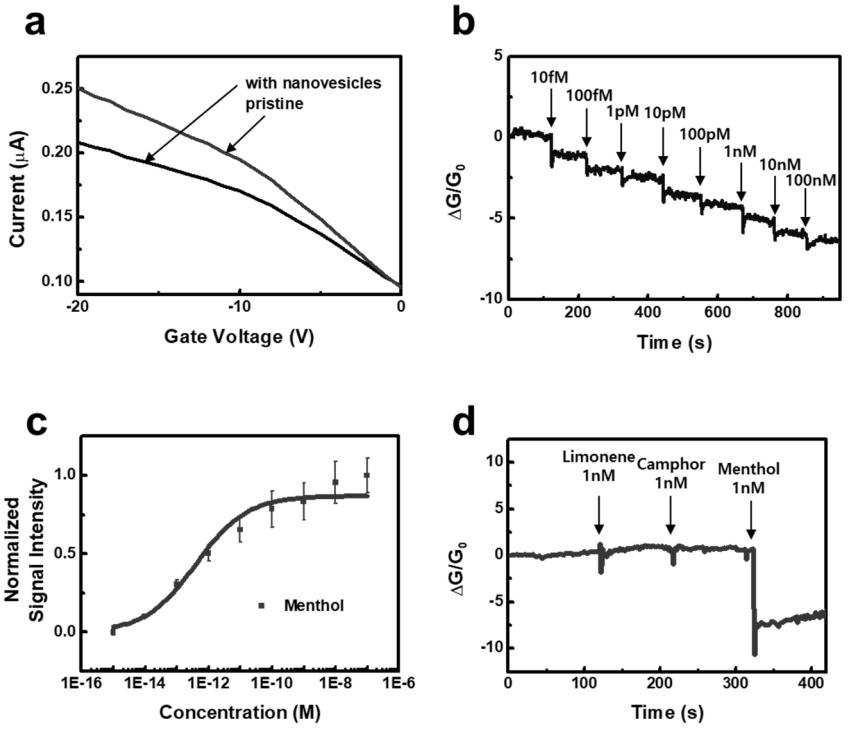

Figure 2-3 Detection of menthol with bioelectronic skins. (a) Gate characteristics of bioelectronic skins before and after immobilization with nanovesicles. The CNT-FETs exhibited p-type characteristics even after immobilization with nanovesicles. (b) Real-time conductance measurement data obtained from chemical cold sensors after the introduction of menthol. The conductance decreased after the introduction of menthol solution with a femtomolar concentration. (c) Dose-dependent responses of bioelectronic sensors. The normalized sensitivity data were obtained by normalizing the sensor sensitivity (|ΔG/G0|) values with respect to the maximum sensitivity value of bioelectronic sensors. For each data point, we repeated the measurement for four devices to obtain the averaged values and error bars. The rather narrow error bars imply that we could obtain reliable responses from our sensors. (d) Real-time conductance measurement data obtained from our

bioelectronic sensors after the introduction of different chemical stimuli. The addition of 1 nM limonene and camphor solutions had no effect on the conductance of the bioelectronic sensor, while the addition of 1 nM menthol solution caused a sharp decrease in the conductance of the bioelectronic sensor.

Figure 2-3a shows the gate profiles of a bioelectronic skin before and after the immobilization of hTRPM8. The devices exhibited typical p-type semiconductor characteristics in both cases, indicating that the electrical characteristics of the devices were maintained even after the immobilization of hTRPM8 on CNT channels. Note that the electrical currents were decreased by the immobilization of hTRPM8. This is presumably because negatively charged parts of receptors immobilized on CNTs caused the gating effect and affected the drain−source currents [25].

Figure 2-3b shows the real-time response to various concentrations of menthol obtained by a bioelectronic skin. A bias voltage of 0.1 V was applied and maintained during electrical measurements. Here, source-drain currents were monitored after the introduction of menthol solutions to the device. As shown in Figure 2-3b, the introduction of menthol solutions resulted in the decrease of FET channel conductance with a dose-dependent manner. Here, the sensor

signal ($\left|{\Delta G}/{G_0}\right|$) represents relative FET channel conductance change at a certain concentration. Our sensor began to respond to menthol at a concentration of 10 fM. However, the sensor without hTRPM8 did not respond to menthol solutions in Figure 2-4, indicating that the bioelectronic skin could respond to menthol in real-time with high sensitivity. The binding of menthol onto the hTRPM8 induced a Ca^{2+} influx into the nanovesicles. Subsequently, the increased concentration of Ca^{2+} in nanovesicles can give a field effect on the underlying CNT-FETs, resulting in the decrease of a channel conductance because CNTs exhibit p-type behaviors under ambient conditions.

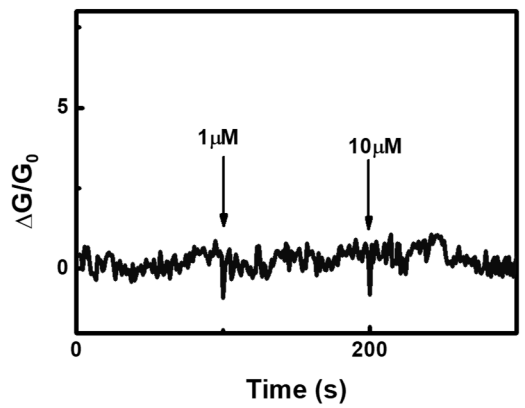

Figure 2-4 Real-time response of the bioelectronic skin without nanovesicles to menthol solutions The sensor did not show changes in conductance even after the introduction of menthol solutions at high concentrations.

Figure 2-3c shows the normalized signals of bioelectronic skins at various concentrations of menthol. The normalized signals of bioelectronic skins to each concentration of menthol solution were obtained through normalizing sensor signals with respect to their maximum signal values at high concentrations [23,24]. We repeated the sensing measurements for four or more bioelectronic skin devices to calculate averaged values and standard deviations. Even though we use devices fabricated in same condition, there is a little bit of a difference in device characteristics, which led to the variation in responses. Rather narrow error bars indicate that we could obtain reproducible and reliable responses from our bioelectronic skins. At 10 fM or higher concentrations, the sensors exhibited normalized signals larger than error bars, indicating that our sensor can detect menthol down to 10 fM.

The normalized signal increased as the concentration of menthol increased, and it was saturated at a high concentration of 100 nM. Here, the dose-dependent responses of the bioelectronic skins can be analyzed by a model based on a Hill equation as reported previously [23-26]. First, we assume that binding events between receptors (hTRPM8) and menthol follow the Hill equation. Then, the density C_s of menthol bound to the receptors can be written as

(1) $$C_s = \frac{C_{s\ max} \cdot C^n}{1/K + C^n}$$

Here, C and K are the concentration of menthol in a solution and an equilibrium constant between the hTRPM8 and menthol, respectively. $C_{s\ max}$ is the density of hTRPM8 on CNT channels, and n is the value of a Hill coefficient. If we assume that a conductance change ΔG is linearly proportional to the number of bound menthol, the sensor signal $\left|\Delta G/G_0\right|$ can be approximated as $\left|\Delta G/G_0\right| \sim kC_s$, where k is a constant representing the response characteristics of a bioelectronic skin. When C becomes very large, the sensor signal $\left|\Delta G/G_0\right|$ converges to the value of $kC_{s\ max}$. Then, we could write the normalized signal N as follows:

(2) $$N = \frac{C^n}{1/K + C^n}$$

By fitting the experimental data using Eq 2, we can estimate the equilibrium constant K between hTRPM8 and menthol as 1.1 x 10^{-12} M. This quantitative analysis also helps us to predict the responses of our bioelectronic skins with the thermoreceptor of the human to its ligand.

Figure 2-3d shows the real-time response of the bioelectronic skins to various chemical stimuli. Limonene and camphor have a similar

structure with menthol. The injections of limonene and camphor with 1 nM concentrations caused negligible conductance changes, while that of 1 nM concentration menthol caused a sharp decrease in the FET channel conductance. This result implies that the bioelectronic skin discriminates menthol from other chemical stimuli with high selectivity.

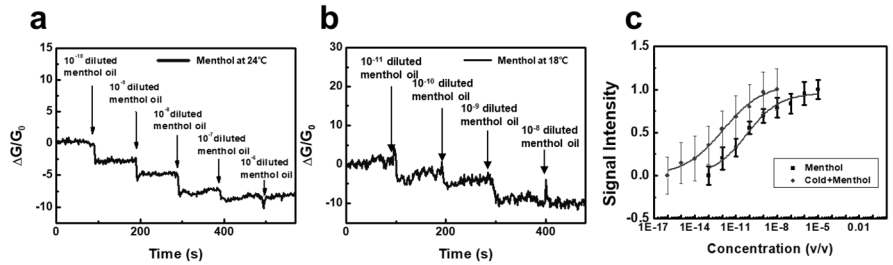

Figure 2-5 Detection of menthol at various temperatures using bioelectronic skins. (a) Real-time responses of a bioelectronic sensor to various concentrations of menthol in menthol oil solutions at 24℃. When diluted menthol oil solutions were introduced, the conductance of a channel decreased in a dose-dependent manner. (b) Real-time responses of bioelectronic skins to menthol in menthol oil solutions at 18℃. (c) Normalized responses of bioelectronic sensors to natural menthol oil at different temperatures.

Thermoreceptor hTRPM8 is also known to be activated by cool sensation (~18℃). To demonstrate the responsiveness to the low temperature of bioelectronic sensors, we also conducted the experiments of detecting menthol in commercial menthol oil samples at different

temperatures. Figure 2-5a and b show the real-time responses of bioelectronic skins to menthol in menthol oil at 24℃ and 18℃, respectively. We added different amounts of menthol oil to PBS buffer solutions and demonstrated that our sensors can detect menthol in natural oil environments at 24℃ and 18℃. For the sensing experiments, drain-source currents of the sensors were measured using a semiconductor analyzer while adding various concentrations of menthol oil solutions. During the measurements, we maintained the temperature of 24℃ and 18℃. The addition of menthol oil solutions to the sensor caused immediate decreases in the conductance of the CNT-FET with hTRPM8 in a dose-dependent manner, while the sensor without nanovesicles did not exhibit conductance changes after the addition of menthol oil solutions (Figure 2-6). The sensor signal began to respond to the addition of menthol oil samples with the diluted concentration of 10^{-10} at 24℃. However, the sensor began to show responses from the diluted concentration of 10^{-11} at 18℃. Presumably, the TRPM8 receptors were activated by only menthol at 24℃, while at low temperature, the TRPM8 receptors were activated by both cool sensation (at 18℃) and menthol, so that the device responded to lower concentration of menthol solutions. The results show that our sensor could detect menthol in natural menthol oil environments and also cool.

Figure 2-5c shows the normalized responses of CNT-FET to menthol oil at different temperatures. The menthol oil was diluted at different ratios with PBS buffer solutions. Each data point was obtained by multiple measurements using four or more bioelectronic skin devices. At 24℃, the sensors began to respond to the addition of menthol oil samples with the diluted concentration of 10^{-10}, and their signals were saturated at the diluted concentration of 10^{-6}. At 18℃, the sensors began to show responses from the diluted concentration of 10^{-11}, and sensor signals were saturated at the diluted concentration of 10^{-5}. The results clearly show that our sensor device responded to menthol as well as to cool sensation. By fitting the dose-dependent response data using Eq. (1), we could estimate equilibrium constant of menthol in the commercial menthol oil at 24℃ as 1.2×10^{-12} M, which is similar to the value in Figure 3-4c [27]. The result clearly indicates that our sensor could quantitatively evaluate menthol in complex environments such as natural-oil products. At 18℃, the equilibrium constant of menthol in menthol oil was estimated as 1.8×10^{-11} M, which was lower than that of menthol oil at 24℃. The result shows the response of thermoreceptor activity was enhanced at lower temperature. It is previously reported that when the temperature is below 18℃, the structure of C-terminal repeat domain of TRPM8 is changed, resulting in the opening of Ca^{2+} ion

channels [28,29]. Presumably, the activity of TRPM8 to menthol was monitored more sensitively by cool stimuli. This results clearly show that the bioelectronic skins could recognize menthol in complex environments such as natural cinnamon oil, and they can be utilized for various applications such as an artificial skin that can recognize chemical cool stimuli.

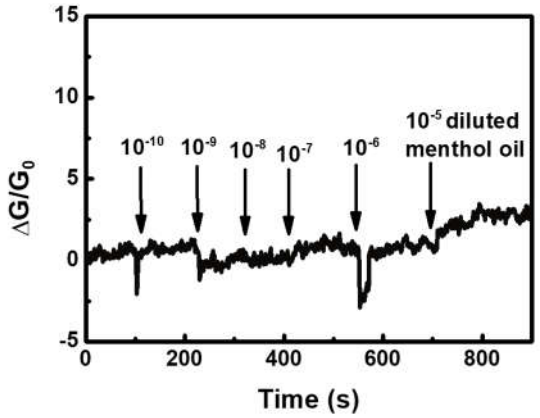

Figure 2-6. Real-time response of the bioelectronic skin without nanovesicles to commercial menthol oil solutions The sensor did not show changes in conductance after the introduction of menthol oil solutions.

2.5 Summary

In summary, we have successfully built a bioelectronic skin imitating human somesthetic systems for the detection of menthol using the hybridization of CNT-FETs and nanovesicles containing human thermoreceptor, hTRPM8. This bioelectronic skin detects menthol down to 10 fM and discriminates between menthol and other chemical stimuli with high sensitivity and selectivity. The bioelectronic skin also perceives the presence of menthol in a real-sample such as menthol oil for electronic cigarette liquid. Importantly, we have demonstrated the enhancement between menthol and cool sensation. Our strategy can overcome the limitation of previous methods in terms of sensitivity and less restrictive experimental conditions. In light of these, a bioelectronic skin imitating human somesthetic systems can be a simple, but highly effective tool in many basic research areas about somesthetic sensory systems.

2.6 References

[1] Robles-De-La-Torre, G., 2006. IEEE Multimedia 13, 24–30.

[2] Chou, M.Z., Mtui, T., Gao, Y.D., Kohler, M., Middleton, R.E., *Biochemistry* **2004**, 43, 2501–2511.

[3] De Maria, G., Natale, C., Pirozzi, S., 2012. Sensors and Actuators A: Physical175, 60–72.

[4] Karimov, K.S., Saleem, M., Karieva, Z.M., Khan, A., Qasuria, T.A., Mateen, A., 2011. Physica Scripta, 83.

[5] Peng, P., Rajamani, R., Erdman, A.G., 2009. Journal of Microelectromechanical Systems 18, 1226–1233.

[6] Suwanratchatamanee, K., Matsumoto, M., Hashimoto, S., 2010. IEEE Transactions on Industrial Electronics 57, 1074–1087.

[7] Thomas V., Grzegorz O., Annelies J., Karel T., Bernd N., *Nat. Chem. Biology* **2007**, 3, 174-182.

[8] Andrea M. P., Aziz M., Anne C. H., Alison J. R., David A. A., Gina M. S., Taryn J. E., Ilaria D., Peter M., Stuart B., Ardem P., *Cell* **2002**, 108, 705-715.

[9] Diana M. B., Jan S., Joshua M. G., Pamela R. T., Allan I. B., Cheryl L. S., Sven-Eric J., David J., *Nature* **2007**, 448, 204-209.

[10] Jin, H.J., Lee, S.H., Kim, T.H., Park, J., Song, H.S., Park, T.H., Hong, S., *Biosensors and Bioelectronics* **2012**, 35, 335–341.

[11] Kim, T.H., Song, H.S., Jin, H.J., Lee, S.H., Namgung, S., Kim, U.K., Park, T.H., Hong, S., *Lab on a Chip* **2011**, 11, 2262–2267.

[12] Kim, T.H., Lee, S.H., Lee, J., Song, H.S., Oh, E.H., Park, T.H., Hong, S., *Advanced Materials* **2009**, 21, 91–94.

[13] Lee, S.H., Kwon, O.S., Song, H.S., Park, S.J., Sung, J.H., Jang, J., Park, T.H., *Biomaterials* **2012**, 33, 1722–1729.

[14] Park, J., Lim, J.H., Jin, H.J., Namgung, S., Lee, S.H., Park, T.H., Hong, S., *Analyst* **2012**, 137, 3249–3254.

[15] Ignacio S., Jianguo G., *Molecular Pain* **2010**, 6, 47.

[16] Ying Y., Mengyu W., Lejla Z., William F. B., Gabriel C. L., Seok Y. L., *Science* **2018**, 359, 237-241.

[17] Lee, M.; Im, J.; Lee, B. Y.; Myung, S.; Kang, J.; Huang, L.; Kwon, Y. K.; Hong, S. *Nat. Nanotechnol.* **2006,** *1*, 66-71.

[18] Park, J.; Lim, J. H.; Jin, H. J.; Namgung, S.; Lee, S. H.; Park, T. H.; Hong, S. *Analyst* **2012,** *137*, 3249-3254.

[19] Kim, T. H.; Lee, S. H.; Lee, J.; Song, H. S.; Oh, E. H.; Park, T. H.; Hong, S. *Adv. Mater.* **2009,** *21*, 91-94.

[20] Kim, B.; Lee, J.; Namgung, S.; Kim, J.; Park, J. Y.; Lee, M. S.; Hong, S. *Sens. Actuators, B* **2012,** *169*, 182-187.

[21] Muhammad A. S., Angela k. V., Daniel B., Leopoldo R. B., Gunter G., Hanns H., *J. Pharm. Pharmaceut Sci*. **2010**, 13, 242-253

[22] Dong, H.; Dunn, J.; Lytton, J. *Biophys. J.* **2002,** *82*, 1943-1952.

[23] Jin, H. J.; An, J. M.; Park, J.; Moon, S. J.; Hong, S. *Biosens. Bioelectron.* **2013,** *49*, 86-91.

[24] Kim, T. H.; Song, H. S.; Jin, H. J.; Lee, S. H.; Namgung, S.; Kim, U. K.; Park, T. H.; Hong, S. *Lab Chip* **2011,** *11*, 2262-2267.

[25] Melinda M. D.; Yifan C.; David J. *Science.* **2019**.

[26] Yoshii, K.; Yokouchi, C.; Kurihara, K. *Brain Res.* **1986,** *367*, 45-51.

[27] Li, X. D.; Staszewski, L.; Xu, H.; Durick, K.; Zoller, M.; Adler, E. *Proc. Natl. Acad. Sci. U. S. A.* **2002,** *99*, 4692-4696.

[28] Christopher B. P.; Rachelle G. *J. Bio. Chem.* **2007,** *50*, 36474-36480.

[29] Sebastian B.; Gerardo O.; Marcelo S.; Eduardo R.; Ramon L., *J. Neurosci.* **2006,** *26*, 4835-4840.

Chapter 3

Bioelectronic Skin based on hTRPA1 in Nanovesicles for the Monitoring of Human Thermoreceptor Activity to Irritant and Cold Sensation

3.1 Introduction

The somesthetic senses in animals include the versatile senses of pressure, temperature and pain [1]. Animals use their somesthetic senses to recognize external environmental changes and avoid danger, which inspired many researchers to develop artificial sensory devices to study and mimic animal senses. Previous research has focused primarily on mechanical or thermosensors, resulting in the development of various artificial devices such as touch pads and thermocouples [2-6]. These senses of temperature and pain are an important part of somesthetic senses, but research on temperature-sensitive tactile sensations has been limited. For example, analytical methods such as cellular calcium assays and electric potential measurements have been used for the detection of chemical stimuli such as cold and pain [7-9]. However, cell-based assays are not suitable for building artificial sensory devices due to the complex pretreatment process and long measurement time. Meanwhile, hybrid nanostructures based on carbon nanotubes and receptor proteins have been used to build artificial sensory devices that mimic the human nose and tongue [10-14]. However, sensor devices for detecting cold-pain stimuli at low temperatures have not yet been developed.

In this dissertation, we built a cold-pain sensor to detect cold and

chemical pain stimuli just like human somesthetic sensory systems. In this work, we expressed a human transient receptor potential ankiryn 1 (hTRPA1), a receptor protein for cold-pain stimuli, in human embryonic kidney cell line 293T (HEK293T) cells, and nanovesicles produced from the cells were immobilized on floating electrode-based single walled carbon nanotube field effect transistors (swCNT-FETs). In human, the hTRPA1 is involved in the transmission and modulation of cold and pain [15,16]. In our sensor device, the nanovesicles containing the hTRPA1 protein responded to cold-pain stimuli, which was monitored electrically via the underlying floating electrodes-based swCNT-FETs. Our cold-pain sensors could selectively detect chemical pain stimuli such as cinnamaldehyde at 1 pM concentration among other chemical stimuli. Furthermore, we utilized our devices to evaluate the effect of cold stimuli on the responses of receptors and found that the receptors responded more sensitively to cinnamaldehyde at a lower temperature than at a higher temperature. This is the first sensor device which allows us to quantitatively measure the cold pain stimuli in real time just like human sensory systems. Our cold-pain sensor should be a powerful platform for a fundamental study regarding somesthetic systems, and it can be also utilized for various practical applications such as drug and food screening.

3.2 Structure of a Bioelectronic Skin Comprised of hTRPA1 in Nanovesicles and a Carbon Nanotube-based Transistor

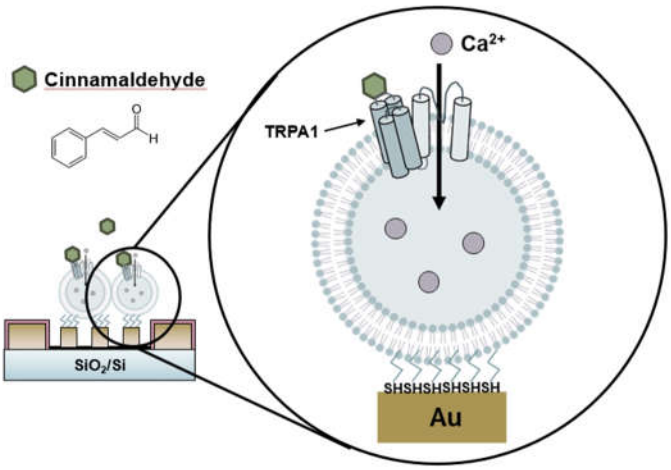

Figure 3-1 Schematic diagram showing the structure of a floating electrode-based bioelectronic skin. The CNT-FET was fabricated by previously-reported processes including a photolithography and a thermal evaporation method. The nanovesicles including hTRPA1 receptors were immobilized on the floating electrode channel. hTRPA1 can respond to specific chemical and cold stimuli with a high selectivity.

Figure 3-1 shows a schematic diagram depicting a hybrid structure of nanovesicles containing a human thermoreceptor and floating electrodes based carbon nanotube field effect transistor (CNT-FET) [17-20]. In brief, single-walled CNTs were selectively adsorbed in channel regions on a SiO_2 substrate via surface-directed assembly strategy, and metal electrodes and floating electrodes were fabricated by

conventional microfabrication. The source-drain electrodes were covered by a passivation layer using photolithography to prevent leakage currents during sensing measurement in aqueous environments. We immobilized the nanovesicles containing hTRPA1 on the floating electrodes of the device. The hTRPA1, human thermoreceptor, could detect cold and pain stimuli. For the sensing experiment, sample solution including pain stimuli, cinnamaldehyde, with different concentrations were applied to a bioelectronic skin device while monitoring the conductance change of the CNT channels in the device. When cinnamaldehyde bound to the trpa1 receptors, it induced a Ca^{2+} influx into the nanovesicles, and the increased concentration of Ca^{2+} in nanovesicles resulted in the increased of the FET channel conductance via the Schottky barrier modulation, allowing us to monitor cinnaladehyde in real-time.

3.3 Characterization of hTRPA1 Expressed in HEK-293 Cells and Nanovesicles

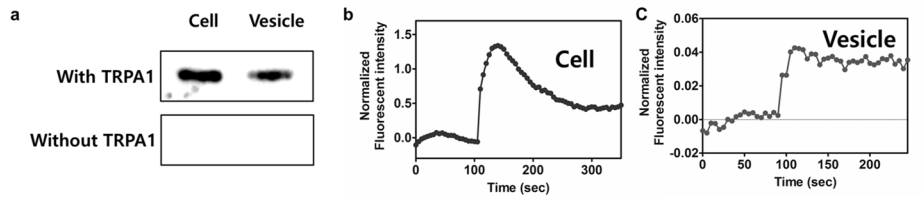

Figure 3-2 Characterization of hTRPA1 expressed in HEK-293 cells and nanovesicles. (a) Western blot analysis of hTRPA1 protein expression in HEK-293T cells and cell-derived nanovesicles. Transfected cells and nanovesicles with hTRPA1 exhibited the specific band corresponding to the molecular weight of hTRPA1, while control cells and nanovesicles (without hTRPA1) did not show the band. (b) Real-time measurement of Ca^{2+} assay in the cells containing hTRPA1. The addition of 10 mM of cinnamaldehyde resulted in the increase of fluorescence intensity. (c) Real-time measurement of Ca^{2+} assay in the nanovesicles containing hTRPA1. The addition of 10 mM of cinnamaldehyde resulted in the increase of fluorescence intensity.

Figure 3-2a shows Western blot analysis for the confirmation of hTRPA1 expression. In brief, the expressions of hTRPA1 protein in HEK-293T cells and cell-derived nanovesicles were confirmed from the lysates of transfected with HEK-293T cells and nanovesicles by Western blot analysis [20-22]. The hTRPA1 antibody is polyclonal and was obtained from rats exposed to a synthetic peptide from the hTRPA1 sequence. Lane 1 represents the data from hTRPA1-expressing cells and nanovesicles derived from them, while lane 2 represents the data from

control cells and nanovesicles. The band of 120 kDa which shows the molecular weight of hTRPA1 was observed from the hTRPA1-expressing cells and cell-derived nanovesicles, while the band was not observed from control cells and nanovesicles [23]. These data indicate that hTRPA1, the human thermoreceptor, was expressed in HEK-293T cells and nanovesicles. In this manner, we determined that the cell derived-nanovesicles contained a sufficient amount of the human thermoreceptor. To investigate the functional activity of hTRPA1, we carried out the measurement of intracellular calcium concentration changes in hTRPA1-expressing HEK-293T cells upon the stimulation of chemical pain stimuli, cinnamaldehyde.

We also performed calcium image analysis to identify whether hTRPA1-mediated Ca^{2+} influx could activate calcium signals in cells. Figure 3-2b shows the real-time measurement of Ca^{2+} assay in nanovesicles containing hTRPA1. Note that treatment of the nanovesicles containing hTRPA1 with cinnamaldehyde (10 mM) resulted in the immediate increase of fluorescence ratio. It indicates that the binding of cinnamaldehyde onto the hTRPA1 induced a Ca^{2+} influx into the cells. In addition, the recovery of calcium signaling to a baseline in the cells was observed, as previously reported [19,24].

Figure 3-2c shows the real-time measurement of Ca^{2+} assay in nanovesicles containing hTRPA1. Note that treatment of the nanovesicles containing hTRPA1 with cinnamaldehyde (10 mM) resulted in the immediate increase of fluorescence ratio. It indicates that the binding of cinnamaldehyde onto the hTRPA1 induced a Ca^{2+} influx into the nanovesicles. These data suggested that functional hTRPA1 was expressed and incorporated into a cell's plasma membrane, and retained its functional response to agonist when isolated in nanovesicles. In this case, the recovery of calcium signaling to a baseline in the nanovesicles was not observed, probably because of the lack of ion pumps and calmodulin which are necessary to restore the Ca^{2+} concentration [19,24].

3.4 Electrical Responses of Bioelectronic Skins

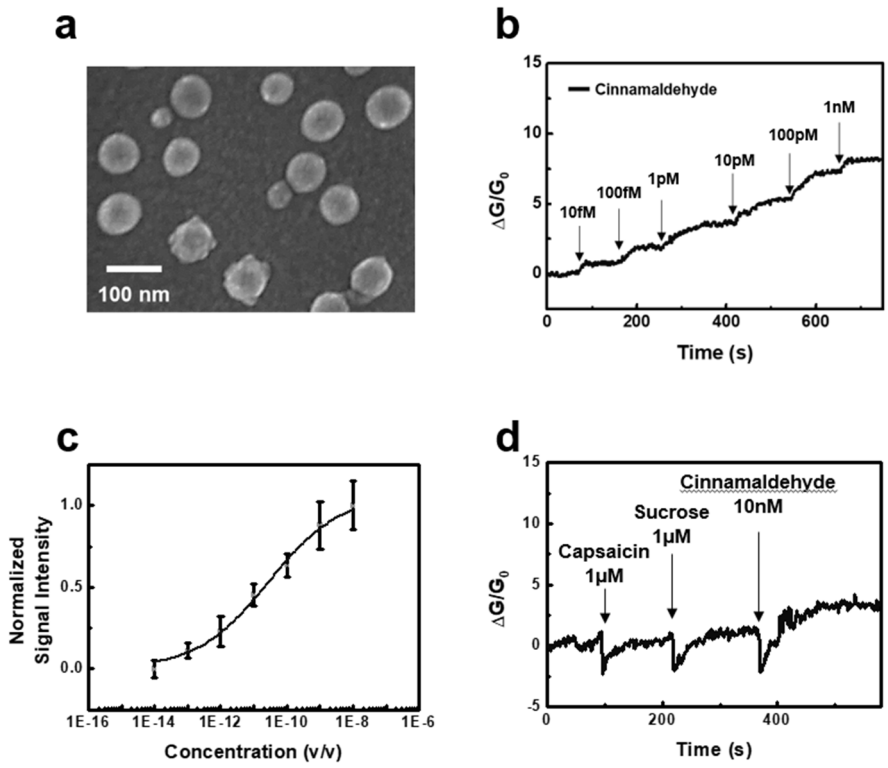

Figure 3-3 Responses of floating electrode-based bioelectronic skins to cinnamaldehyde solutions. (a) FE-SEM image of nanovesicles containing hTRPA1 on the gold substrate. (b) Real-time electrical measurement of cinnamaldehyde. The introduction of cinnamaldehyde caused an increase in the FET channel conductance. The FET channel conductance began to increase after the addition of cinnamaldehyde with 1 pM. (c) Dose-dependent responses of floating electrode-based bioelectronic skins to cinnamaldehyde. The normalized signal increased as the concentration of cinnamaldehyde increased, and it was saturated at around 1 nM. We repeated sensing measurements for four or more bioelectronic skin devices to confirm the reliability. The error bars represent the standard deviations of the normalized sensor signals. (d) Real-

time electrical response of a floating electrode-based bioelectronic sensor to various chemical stimuli. The conductance of the sensor negligibly changed during the adding of sucrose and capsaicin, while the injection of cinnamaldehyde resulted in a large increase in its channel conductance.

Figure 3-3a shows the field emission scanning electron microscopy image of nanovesicles fixed on a gold floating electrode. To maintain the structure of nanovesicles, the nanovesicles immobilized on the gold surface were lyophilized using a freeze dryer. Then, the surface was covered with platinum (5 nm) by a sputtering system. The nanovesicles ranged in diameter from 80 nm to 100 nm. This clearly shows that we successfully constructed nanovesicles with optimized sizes and could immobilized them uniformly on gold surfaces [25].

Figure 3-3b shows the real-time response of a floating electrode-based bioelectronic skin device to various concentrations of cinnamaldehyde in aqueous environments. For the measurement, 9 μL of phosphate buffered saline (PBS) was first placed on the channel region of a bioelectronic skin sensor. Then, the source-drain current in the channel was monitored during the addition of cinnamaldehyde solutions with different concentrations ranging from 1 fM to 1 nM. Here, the

relative conductance change |⊿G/G0| of the floating electrode based CNT-FET channel at a certain concentration was used as a sensor signal [26]. The sensor signal began to increase at a concentration of 1 fM. Note that the bare floating electrode based CNT-FET without hTRPA1 did not exhibited conductance changes by the addition of cinnamaldehyde solutions (Figure 3-4). These results indicate that the sensor responses came from the specific binding between cinnamaldehyde and hTRPA1 on the floating electrode based CNT-FET channel. A plausible explanation is that the binding of cinnamaldehyde onto the hTRPA1 induced a Ca^{2+} influx into the nanovesicles. Subsequently, the increased concentration of Ca^{2+} in nanovesicles resulted in the increase of the FET channel conductance *via* the Schottky barrier modulation between the CNT networks and the floating electrodes [25].

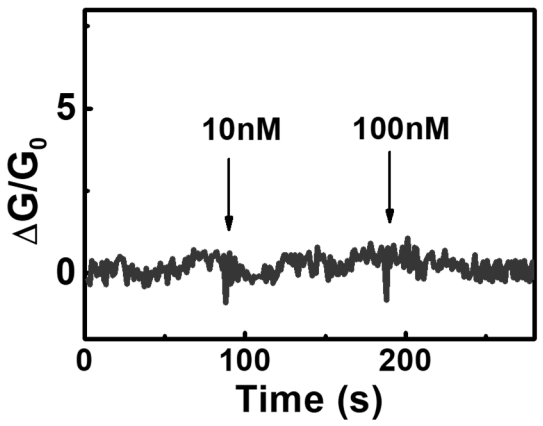

Figure 3-4 Real-time response of the bioelectronic skin without nanovesicles to cinnamaldehyde solutions The sensor did not exhibit changes in conductance even after the introduction of cinnamaldehyde solutions at high concentrations.

Figure 3-3c displays the normalized responses of floating electrode-based bioelectric skin devices to cinnamaldehyde at different concentrations. Here, the normalized responses were calculated by normalizing sensor signals with respect to their maximal sensor signal values at high concentration conditions [25-27]. The measurement at a single concentration was carried out repeatedly using four or more bioelectronic skin devices to obtain average values and standard errors. Our sensors began to show responses from the concentration of 1 fM, and the responses were almost saturated around 1 nM. Note that the error bars were much smaller than the sensor signals from the concentration of 1 fM, indicating the reliable detection of cinnamaldehyde with a high sensitivity.

The dose-dependent responses of our bioelectronic skin sensors were analyzed by the Hill equation as reported previously [25-27]. Previous works showed that the normalized signal N of bioelectronic skin devices based on a CNT-FET could be written like

$$N = \frac{C^n}{\frac{1}{K}+C^n} \quad (1)$$

where *C, K and n* are the *concentration of cinnamaldehyde solution*, the *equilibrium constant for the binding of the cinnamaldehyde to hTRPA1 receptors* and *a Hill's coefficient*, respectively. The fitting of the normalized sensor signals by Eq. (1) allowed us to estimate the equilibrium constant *K* between cinnamaldehyde and hTRPA1 receptors as ~4.7×10^{-11} M in the cinnamaldehyde solution with PBS. The estimated *K* value is rather large compared with previously reported value measured using cell-based fluorescence assays [15]. The result shows that our bioelectronic sensors can detect cinnamaldehyde at much lower concentrations than those of cell-based sensing systems. Similar trends were also reported in case of other bioelectronic sensor devices [25,27]. The plausible explanation may be that our device could directly detect the binding of receptor proteins without any intermediate biological steps, increasing the sensitivity of our method. However, the cell-based fluorescence assays relied on complicated signal transduction steps inside the cell. In this case, such intermediate steps in cell-based biological systems require several different materials other than cinnamaldehyde to generate sensing signals, which could result in a rather low sensitivity of the cell-based biological systems. The Hill

coefficient n was estimated as 0.4 for the binding of cinnamaldehyde to hTRPA1 in nanovesicles. Note that the low Hill coefficient ($n < 1$) implies the negatively-cooperative binding of cinnamaldehyde to hTRPA1. Presumably, it is because of the possible aggregation and steric hindrance of receptor proteins on our bioelectronic sensor devices [28].

Figure 3-3d displays the real-time response of a floating electrodes-based bioelectronic sensor to various substances. Here, we consecutively added the 1 μM solutions of capsaicin, sucrose and the 1 pM solution of cinnamaldehyde to the floating electrodes-based bioelectronic sensor while measuring the sensor responses. The capsaicin and sucrose are stimulating substances. Note that the addition of capsaicin and sucrose solutions with 1 μM concentrations caused the negligible conductance changes, while the addition of a diacetyl solution with a 1 pM concentration sharply increased the conductance of the CNT channel in the sensor. The result clearly shows that our floating electrodes-based bioelectronic skin could discriminate cinnamaldehyde from other similar molecular species with a high selectivity.

3.5 Detection of Cinnamon Oil Ingredients with Different Temperatures

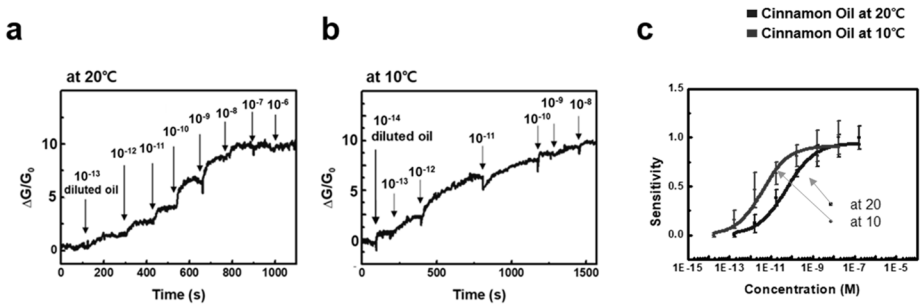

Figure 3-5 Detection of cinnamaldehyde at various temperatures using floating electrode-based bioelectronic skins. (a) Real-time responses of a floating electrode-based bioelectronic sensor to various concentrations of cinnamaldehyde in cinnamon oil solutions at 20℃. When diluted cinnamon oil solutions were introduced, the conductance of a channel increased in a dose-dependent manner. (b) Real-time responses of floating electrode-based bioelectronic skins to cinnamaldehyde in cinnamon oil solutions at 10℃. (c) Normalized responses of floating electrode-based bioelectronic sensors to natural cinnamon oil at different temperatures.

Thermoreceptor hTRPA1 is also known to be activated by cold stimuli (<17℃) [15]. To demonstrate the responsiveness to the low temperature of a floating electrode-based bioelectronic sensor, we also conducted the experiments of detecting cinnamaldehyde in commercial cinnamon oil samples at different temperatures. Figure 3-5a and b show the real-time responses of a floating electrode-based bioelectronic skin to cinnamaldehyde in cinnamon oil at 20℃ and 10℃, respectively. We

added different amounts of cinnamon oil to PBS buffer solutions and demonstrated that our sensors can detect cinnamaldehyde in natural oil environments at 20℃ and 10℃. For the sensing experiments, drain-source currents of the sensors were measured using a semiconductor analyzer while adding various concentrations of cinnamon oil solutions. During the measurements, we used dry ice to maintain a temperature of 10℃. The addition of cinnamon oil solutions to the sensor caused immediate increases in the conductance of the floating electrode-based CNT-FET with hTRPA1 in a dose-dependent manner, while the sensor without nanovesicles did not exhibit conductance changes after the addition of cinnamon oil solutions (Figure 3-6). The sensor signal began to respond to the addition of cinnamon oil samples with the diluted concentration of 10^{-13} at 20℃. However, the sensor began to show responses from the diluted concentration of 10^{-14} at 10℃. Presumably, the hTRPA1 receptors were activated by only cinnamaldehyde at 20℃, while at low temperature, the hTRPA1 receptors were activated by both cold (at 10℃) and cinnamaldehyde, so that the device responded to lower concentration of cinnamaldehyde solutions [15,29]. The results show that our sensor could detect cinnamaldehyde in natural cinnamon oil environments and also cold.

Figure 3-5c shows the normalized responses of floating electrodes based CNT-FET to cinnamon oil at different temperatures. The cinnamon oil was diluted at different ratios with PBS buffer solutions. Each data point was obtained by multiple measurements using four or more bioelectronic skin devices. At 20℃, the sensors began to respond to the addition of cinnamon oil samples with the diluted concentration of 10^{-13}, and their signals were saturated at the diluted concentration of 10^{-3}. At 10℃, the sensors began to show responses from the diluted concentration of 10^{-14}, and sensor signals were saturated at the diluted concentration of 10^{-1}. The results clearly show that our sensor device responded to cinnamaldehyde as well as to cold stimuli. By fitting the dose-dependent response data using Eq. (1), we could estimate equilibrium constant of cinnamaldehyde in the commercial cinnamon oil at 20℃ as 5.2×10^{-11} M, which is similar to the value in Figure 3-5c. The result clearly indicates that our sensor could quantitatively evaluate cinnamaldehyde in complex environments such as natural-oil products. At 10℃, the equilibrium constant of cinnamaldehyde in cinnamon oil was estimated as 1.8×10^{-11} M, which was lower than that of cinnamon oil at 20℃. The result shows the response of tactile receptor activity was enhanced at lower temperature. It is previously reported that when the temperature is below 17℃, the structure of N-terminal ankyrin repeat domain of hTRPA1 is changed,

resulting in the opening of Ca^{2+} ion channels [15]. Presumably, the activity of hTRPA1 to cinnamaldehyde was monitored more sensitively by cold stimuli. This results clearly show that the bioelectronic skins could recognize cinnamaldehyde in complex environments such as natural cinnamon oil, and they can be utilized for various applications such as an artificial skin that can recognize cold and pain stimuli.

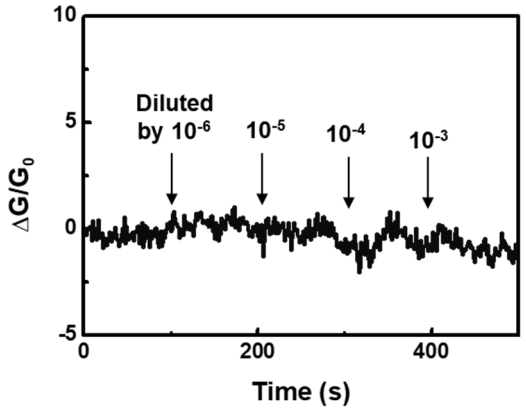

Figure 3-6 Real-time response of the bioelectronic skin without nanovesicles to commercial cinnamon oil solutions The sensor did not exhibit changes in conductance even after the introduction of commercial cinnamon oil solutions at high concentrations.

3.6 Summary

In summary, we have successfully developed a floating electrode-based bioelectronic skin mimicking human somesthetic systems for the detecting of cold and chemical pain stimuli using the hybridization of floating electrode-based CNT-FETs and nanovesicles containing human thermoreceptors, hTRPA1. This bioelectronic skin recognizes chemical stimuli, cinnamaldehyde, down to 1 pM and discriminates between cinnamaldehyde and other chemical stimuli with a high sensitivity and selectivity. Also, we utilized our devices to evaluate the effect of cold stimuli on the responses of receptors and found that the receptors responded more sensitively to cinnamaldehyde at lower temperatures than at higher temperatures. Our cold-pain sensor should be a powerful platform for a fundamental study regarding cold-pain sensory systems, and it can be also utilized for various practical applications such as drug and food screening.

3.7 References

[1] Robles-De-La-Torre, G., 2006. IEEE Multimedia 13, 24–30.

[2] Chou, M. Z., Mtui, T., Gao, Y.D., Kohler, M., Middleton, R.E., *Biochemistry* **2012**, 43, 2501–2511.

[3] De Maria, G., Natale, C., Pirozzi, S., 2012. Sensors and Actuators A: Physical175, 60–72.

[4] Karimov, K.S., Saleem, M., Karieva, Z.M., Khan, A., Qasuria, T.A., Mateen, A., 2011. Physica Scripta, 83.

[5] Peng, P., Rajamani, R., Erdman, A.G., 2009. Journal of Microelectromechanical Systems 18, 1226–1233.

[6] Suwanratchatamanee, K., Matsumoto, M., Hashimoto, S., 2010. IEEE Transactions on Industrial Electronics 57, 1074–1087.

[7] Thomas V., Grzegorz O., Annelies J., Karel T., Bernd N., *Nat. Chem. Biology* **2007**, 3, 174-182.

[8] Andrea M. P., Aziz M., Anne C. H., Alison J. R., David A. A., Gina M. S., Taryn J. E., Ilaria D., Peter M., Stuart B., Ardem P., *Cell* **2002**, 108, 705-715.

[9] Diana M. B., Jan S., Joshua M. G., Pamela R. T., Allan I. B., Cheryl L. S., Sven-Eric J., David J., *Nature* **2007**, 448, 204-209.

[10] Jin, H.J., Lee, S.H., Kim, T.H., Park, J., Song, H.S., Park, T.H., Hong, S., *Biosensors and Bioelectronics* **2012**, 35, 335–341.

[11] Kim, T.H., Song, H.S., Jin, H.J., Lee, S.H., Namgung, S., Kim, U.K., Park, T.H., Hong, S., *Lab on a Chip* **2011**, 11, 2262–2267.

[12] Kim, T.H., Lee, S.H., Lee, J., Song, H.S., Oh, E.H., Park, T.H., Hong, S., *Advanced Materials* **2009**, 21, 91–94.

[13] Lee, S.H., Kwon, O.S., Song, H.S., Park, S.J., Sung, J.H., Jang, J., Park, T.H., *Biomaterials* **2012**, 33, 1722–1729.

[14] Park, J., Lim, J.H., Jin, H.J., Namgung, S., Lee, S.H., Park, T.H., Hong, S., *Analyst* **2012**, 137, 3249–3254.

[15] Lavanya M., Sabeen S., Mohamed K., Charlotte S., Per K., Edward D. H., Urban J., Peter M. Z., *PNAS* **2014**, 111, 16907-16906.

[16] Abdul S., Lucie S., Jan B., Rudiger E., Babak M., Jan T., Viktorie V., *Biochem. J.* **2011**, 433, 197-204.

[17] Lee, M.; Im, J.; Lee, B. Y.; Myung, S.; Kang, J.; Huang, L.; Kwon, Y. K.; Hong, S. *Nat. Nanotechnol.* **2006,** *1*, 66-71.

[18] Park, J.; Lim, J. H.; Jin, H. J.; Namgung, S.; Lee, S. H.; Park, T. H.; Hong, S. *Analyst* **2012,** *137*, 3249-3254.

[19] Kim, T. H.; Lee, S. H.; Lee, J.; Song, H. S.; Oh, E. H.; Park, T. H.; Hong, S. *Adv. Mater.* **2009,** *21*, 91-94.

[20] Letizia A., Jose J. L., Natalia D., Tarik S., Gines M. S., Juan A. R. *J. bbam. mcr.* **2013,** *1833*, 3025-3034.

[21] Xiao-Lei W., Li-Wei C., Ling-Jia B. S. *Neural Regen. Res.* **2019**, 14, 140-148.

[22] Tahrin M., Ping-Chang Y. *N. Am. J. Med. Sci.* **2012,** *4*, 429-434.

[23] De-Shou C., Linlin Z., Tsung-han H., Mruvil A., Mahendra B., Lauren H., Louis S. P. Plos one 2012, 7, 1-10.

[24] Kim, T. H.; Song, H. S.; Jin, H. J.; Lee, S. H.; Namgung, S.; Kim, U. K.; Park, T. H.; Hong, S. *Lab Chip* **2011,** *11*, 2262-2267.

[25] Minju L., Je Won J., Daesan K., Young-Joon A., Seounghun H., Hyung Wook K. *ACS Nano* **2015,** 9, 11728.

[26] Heehong Y., Daesan K., Jeongsu K., Dongseok M., Hyun Seok S., Minju L., Seunghun H., Tai Hyun P. *ACS Nano* **2017,** 11, 11847.

[27] Hye Jun J., Jeong Mi A., Juhun P., Seok Jun M., Seunghun H. *Biosens. and Bioelec.* **2013,** *49*, 86-91.

[28] Minju L., Heehong Y., Daesan K., Myungjae Y., Tai Hyun P., Seunghun H. *Scientific Reports.* **2018,** 8, 13945.

[29] Yuji K., Karel T., Wouter E., Annelies J., Kelvin Y. K., Rudi V., Bernd N., Thomas V. *PNAS* **2009,** 4, 1273-1278.

Chapter 4

Conclusions

In this dissertation, bioelectronic sensors based on CNT-FETs and thermoreceptors were developed to monitor thermoreceptor activity.

Firstly, we developed bioelectronic skins based on nanovesicles to monitor human thermoreceptor activity to menthol. Using the strategy, we quantitatively monitored the thermoreceptor (hTRPM8) activity to menthol even in real samples. The results show that the bioelectronic skins could discriminate menthol with high sensitivity and selectivity. Significantly, we demonstrated that the responses of hTRPM8 to menthol could be enhanced by decreasing temperatures. The results imply that we could quantitatively evaluate the menthol ingredients in real menthol oil and effects of cool sensation using the bioelectronic skins.

Secondly, we developed bioelectronic skins based on nanovesicles to monitor human thermoreceptor activity to cold and pain stimuli. Importantly, we quantitatively discriminated cinnamaldehyde component from the other chemical stimuli. We also quantitatively evaluated the enhancing effect of low temperature to cinnamaldehyde using the bioelectronic skins. Furthermore, the concentration of

cinnamaldehyde, main component of a real-cinnamon oil, was estimated to be close to the actual concentration.

The results should contribute to broadening the understanding of thermoreceptor activity. Further, the development of the bioelectronic sensors should provide a powerful platform mimicking real somesthetic systems. In addition, it is expected to be widely utilized as a practical tool for various applications in general.

Chapter 5

Abstract in Korean

초록

온도 수용체의 작용을 연구하기 위한 나노베지클-탄소나노튜브 융합 장치 및 바이오전자 피부로의 응용

인간은 후각과 미각 촉각 등 다양한 기관을 통해 외부의 냄새, 맛 물질과 온도의 변화를 인지한다. 그 중, 촉각은 피부세포에 존재하는 온도 수용체들이 세포 밖의 화학 신호를 받아들임으로써 생성된다. 즉, 온도 수용체들이 감각 기관에서 첫번째 감지 파트로서 작용하게 된다. 따라서, 온도 수용체의 작용을 측정하는 것은 촉각 기관에 대한 근본적인 이해를 위하여 필수적이다. 또한, 촉각 수용체에 대한 연구는 바이오전자 센서의 개발로 이어질 수 있다. 본 연구에서는 바이오전자 센서를 통하여 촉각 수용체의 작용을 전기적으로 모니터링하는 것에 대

하여 논의 할 것이다. 이 바이오전자 센서는 탄소나노튜브를 채널로 제작한 전계 효과 트랜지스터를 기반으로 하고 있으며, 이 센서는 향상된 센서 감도와 선택성을 가지고 있다.

먼저, 시원한 온도에 대한 인간의 온도 수용체의 작용을 모니터링하기 위한 나노베지클 기반 바이오 전자 촉각 센서에 대하여 논의할 것이다. 이를 위하여, 탄소나노튜브 전계 효과 트랜지스터와 TRPM8 (Transient receptor potential melastatin 8)이라는 인간의 온도 수용체를 포함하고 있는 나노베지클이 융합되었다. 이를 통해 시원한 감각을 내는 물질로 잘 알려진 멘솔 (menthol)을 다른 자극성 물질로부터 높은 감도와 선택성을 가지고 구별할 수 있었다. 흥미롭게도, 이 바이오전자 촉각 센서는 피부에 직접 바르는 마사지 오일에 존재하는 멘솔을 검지하는 데에도 이용되었다.

다음으로, 유해한 차가운 감각 및 고통에 대한 인간의 촉각 수용체의 작용을 모니터링하기 위한 나노베지클 기반 바이오 전자 촉각 센서에 관하여 논의 할 것이다. 이를 위하여, 플로팅 전극 기반의 탄소나노튜브 전계 효과 트랜지스터가 인간 촉각 수용체 TRPA1 (Transient receptor potential

ankiryn 1)가 내장된 나노베지클이 준비되었다. 이를 통해 시나몬의 주요 구성 성분인 신남알데하이드를 1 fM 의 낮은 농도까지 검지할 수 있었다. 우리는 또한 사람의 피부처럼 고통을 느끼는 감각에 대해 차가운 온도인 10도정도에서 반응이 크게 향상됨을 입증하였다. 뿐만 아니라, 이 방법은 시나몬 오일과 같은 실제 샘플에서도 신남알데하이드 성분을 정량적으로 검출하기 위해 사용될 수도 있었다.

주요어: 감각 수용체, 나노베지클, 탄소나노튜브 전계 효과 트랜지스터, 플로팅 전극, 바이오전자 센서

학번: 2015-30092

Acknowledgement

우선 오랜 학위 과정 동안 가르침을 주신 홍승훈 교수님께 큰 감사를 드립니다. 교수님의 제자로서 연구의 기본 자세, 연구 주제를 정하고 진행하는 방법, 그리고 논문을 쓰는 역량까지 말로 다 할 수 없는 가르침을 받은 것 같습니다. 그간 베풀어주신 가르침과 지원에 다시 한 번 감사드리며 끊임없이 발전하도록 항상 노력하겠습니다.

2013년부터 지금까지 연구실에서 생활하고 연구하면서 많은 도움을 주셨던 분들께 감사 인사를 드립니다. 처음 실험실 들어 왔을 때 실험에 대해 잘 알려주고 도와주던 혜준오빠, 주훈오빠와, 그리고 실험실 들어왔을 때 바로 졸업을 하셔서 짧은 시간을 함께한 형우오빠, 중국어와 영어를 잘해서 부러운 세홍씨, 조용히 할 일을 잘하는 동준오빠, 항상 모든 일에 솔선수범하던 동국오빠, 교수님이 그리워 HND로 돌아온 정수오빠, 연구실의 바리스타 대산오빠, 연구를 잘해서 배울 점이 많았던 덕형오빠, 주말 출근을 마다 않는 Shekhar 박사님, 포닥으로 좋은 모습을 보여주셨던 Thao 박사님과 Chen 박사님, 빨리 먼저 졸업해버린 동기 민주. 좋은 분들이 많이 도와주셔서 학교에서의 생활을 무사히 마칠 수 있었습니다.

오랜 시간 연구실의 힘이 되어준 진희언니, 조교장을 병행하며 많은 도움을 주던 하늘 오빠, 어느새 교수님이 된 연구 잘하는 Viet Anh, 여러가지 기구로 운동을 전파하던 영탁이, 글로벌한다고 고생하던 중현이, 새로 들어와서 노이즈연구에 잘 적응한 지혜와 혜송이, 연구를 항상 열심히 하는 윤지, 방장을 넘겨 받아 많은 일로 고생하는 진영오빠, 창업으로 떼돈 벌 인경오빠. 연구실 내 많은 분들의 도움으로 연구실 생활을 무사히 마칠 수 있었습니다. 그 밖에 심적으로 기댈 수 있었던 정난주 교수님, 공동 연구를 진행하며 논문을 쓰는데 큰 도움을 주신 박태현 교수님과 이승환 교수님께 감사의 말씀을 드립니다.

동기로 만났지만 평생 친구로 지내고 싶은 쥴리, 인욱, 동욱, 준영 그리고 소윤언니. 덕분에 즐거웠습니다. 거의 15년을 함께한 내 소중한 친구들 경선, 미림, 주영, 선문, 한나, 지영, 윤정, 지원이 앞으로도 잘 지내자. 언제나 반가운 대학교 친구들 이슬, 연정, 선영이도 이제는 더 자주 만나자. 알게 된 기간은 짧지만 앞으로 사돈을 맺기로 한 재원, 멀리 이사 가서 아쉬운 광민이. 앞으로 더 자주 보자~~

마지막으로 가장 소중한, 항상 제 뒤에서 응원해주신 아빠, 엄마. 항상 사랑합니다. 앞으로 평생 손을 잡고 함께 갈 내 반쪽 성수, 앞으로도 서로 잘 의지하면서 살아가보자. 사랑해.

이제 앞으로 사회로 나갈 동생 성호, 힘 내. 많은 도움을 받아온 만큼, 사랑하는 우리 가족 항상 행복하고 즐거울 수 있도록 이제는 제가 도움이 되고자 하는 바람입니다. 고맙고 사랑합니다.

2020. 01. 23.

신나래 올림